J. Microbiol. Biotechnol. (2017), 27(4), 731–738
https://doi.org/10.4014/jmb.1610.10019

jmb

Canna edulis Leaf Extract-Mediated Preparation of Stabilized Silver Nanoparticles: Characterization, Antimicrobial Activity, and Toxicity Studies

S. V. Otari[1,2], S. H. Pawar[2], Sanjay K. S. Patel[1], Raushan K. Singh[1], Sang-Yong Kim[3], Jai Hyo Lee[4], Liaoyuan Zhang[5*], and Jung-Kul Lee[1*]

[1]*Department of Chemical Engineering, Konkuk University, Seoul 05029, Republic of Korea*
[2]*Center for Interdisciplinary Research, D. Y. Patil University, Kolhapur-416 006, Maharashtra State, India*
[3]*Department of Food Science and Biotechnology, Shin-Ansan University, Ansan 15435, Republic of Korea*
[4]*Department of Mechanical Engineering, Konkuk University, Seoul 05029, Republic of Korea*
[5]*Key Laboratory of Biopesticide and Chemical Biology, Ministry of Education, College of Life Sciences, Gutian Edible Fungi Research Institute, Fujian Agriculture and Forestry University, Fuzhou, Fujian Province 350002, P.R. China*

Received: October 10, 2016
Revised: December 17, 2016
Accepted: January 11, 2017

First published online
January 12, 2017

**Corresponding authors*
J.-K.L.
Phone: +82-2-450-3505;
Fax: +82-2-458-3504;
E-mail: jkrhee@konkuk.ac.kr
L.Z.
Phone: +86-591-83789492;
Fax: +86-591-83789121;
E-mail: zliaoyuan@126.com

pISSN 1017-7825, eISSN 1738-8872

A novel approach to synthesize silver nanoparticles (AgNPs) using leaf extract of *Canna edulis* Ker-Gawl. (CELE) under ambient conditions is reported here. The as-prepared AgNPs were analyzed by UV-visible spectroscopy, transmission emission microscopy, X-ray diffraction, Fourier transform-infrared spectroscopy, energy-dispersive analysis of X-ray spectroscopy, zeta potential, and dynamic light scattering. The AgNPs showed excellent antimicrobial activity against various pathogens, including bacteria and various fungi. The biocompatibility of the AgNPs was analyzed in the L929 cell line using NRU and MTT assays. Acridine orange/ethidium bromide staining was used to determine whether the AgNPs had necrotic or apoptotic effects on L929 cells. The concentration of AgNPs required for 50% inhibition of growth of mammalian cells is far more than that required for inhibition of pathogenic microorganisms. Thus, CELE is a candidate for the eco-friendly, clean, cost-effective, and non-toxic synthesis of AgNPs.

Keywords: Green chemistry, *Canna edulis* Ker-Gawl., nanobiotechnology, antimicrobial, biocompatible

Introduction

Standard "green" science methods, which decrease the utilization or production of dangerous substances, are also being applied in the field of nanoscience, including the synthesis of nanoscale items, leading to the advancement of techniques for creation of nanomaterials [1–4]. A number of chemical and physical methods have been used to synthesize metal nanoparticles, including chemical reduction [5, 6], electrochemical reduction [7–9], photochemical reduction [10], radiation [11, 12], and heat evaporation [13, 14]. However, the chemicals used in these processes are often costly, toxic, and not eco-friendly. In addition, various organic coatings are used to prevent the aggregation of nanoparticles and increase their biocompatibility. When used in large-scale production, these organic coatings may become organic pollutants [15]. Therefore, biological synthesis of nanoparticles has received increasing attention recently, as it is cost effective, clean, eco-friendly, and non-toxic; biological synthesis involves the use of biological entities and non-hazardous chemicals for synthesis of nanomaterials, to minimize or avoid undesirable byproducts. Various prokaryotes and eukaryotes have been used for the synthesis of nanoparticles [16]. Of the numerous nanomaterials being produced, those made with noble metals have garnered significant attention owing to their

optoelectric properties, and have been shown to be exceedingly adaptable and tunable materials for a wide range of applications, including biophysical conjugates, biological detection, imaging, and cancer treatment. Silver nanoparticles (AgNPs) have been studied widely and have been shown to have powerful antimicrobial properties for the treatment of infections, for food preservation, and for water treatment [17]. AgNPs are now being used in medical devices, optical devices, electronics, biotechnological applications, and as biosensors and catalysts [18, 19]. Among the various methods for AgNP synthesis, plant-mediated synthesis has received much attention, as it is very easy and rapid compared with the tedious and time-consuming processes required for microbial synthesis. The extracts of various plant parts, such as calluses, leaves, flowers, fruits, and seeds, have been used for AgNP biosynthesis [20, 21].

In the present work, we demonstrated the biosynthesis of AgNPs using the flowering plant *Canna edulis* Ker-Gawl. *C. edulis* is a tropical herb that grows from a rhizome, with banana-like leaves and multicolored flowers. Many parts of *Canna* spp. are used to regain energy, as a demulcent to stimulate menstruation, to treat suppuration, to treat rheumatism, and as a diuretic in fevers and dropsy, and in traditional medicine as a diaphoretic [22]. Extracts of *C. indica* L. also show antitumor activity in rodents, low toxicity in cell culture, and antimicrobial activity [23]. In addition, *Canna* spp. have been used in built wetlands for removal of organic pollutants, heavy metals, and phosphorus [24]. Although *Canna* spp. have medicinal as well as environmental applications, they have yet to be investigated for use in the biosynthesis of AgNPs. Herein, aqueous leaf extracts of *C. edulis* species (CELE) were used for reduction of aqueous $AgNO_3$ to AgNPs. The AgNPs demonstrated antimicrobial activity against drug-resistant human pathogenic microorganisms. The cytotoxicity of the AgNPs was also studied in a mammalian cell line (L929) using NRU and MTT assays. Finally, acridine orange/ethidium bromide (AO/EB) nuclear staining was used to determine the apoptotic and necrotic effects of the AgNPs on the cell line under a fluorescence microscope.

Materials and Methods

Synthesis of AgNPs

C. edulis Ker-Gawl. leaves were washed under tap and distilled water. The leaves (15 g) were chopped in small pieces and kept in 100 ml double distilled water for 10 min at 50°C. The leaf extract was filtered through nylon cloths and then through Whatman filter papers. The extract was kept at 4°C for 24 h and then used for further experiments.

In 500 ml Erlenmeyer flasks, 10 ml CELE was added to the 90 ml of 2 mM $AgNO_3$ solution and incubated for 24 h at 25°C in dark condition. The effect of different parameters such as $AgNO_3$ concentration, leaf extract concentration, and temperature was studied to maximize production of nanoparticles. To observe effect of $AgNO_3$ concentration on AgNPs synthesis, 10 ml of CELE was added in Erlenmeyer flasks (500 ml) containing 90 ml of 2, 4, and 6 mM aqueous $AgNO_3$. In 100 ml of 10% CELE, different concentration of $AgNO_3$ was added to observe the effect of aqueous $AgNO_3$ on synthesis process. To demonstrate the effect of leaf extract concentrations on AgNPs synthesis, 10, 30, and 50 ml CELE were added in 500 ml Erlenmeyer flasks containing 90 ml of 2 mM aqueous $AgNO_3$ solution. The effects of various temperature (30°C to 60°C) and pH (5 to 9) on the synthesis of AgNPs were also analyzed using 10 ml CELE and 90 ml of 2 mM aqueous $AgNO_3$. For pH adjustment, 1 N NaOH and 1 N HCl were used. The color change was observed after 24 h of incubation and AgNPs synthesis was analyzed using UV-Vis spectrophotometer [17, 29, 30, 32].

Characterization of AgNPs

To verify biosynthesis of AgNPs, UV-visible (UV-Vis) spectroscopy was used (UV 1800; Shimadzu, Japan); AgNPs show a characteristic peak between 400 and 500 nm. The crystalline structure of the as-prepared AgNPs was analyzed using a Philips PW-3710 diffractometer with Cu K_α radiation. XRD patterns were measured using the X'pert high-score software. Freeze-dried leaf extracts were analyzed using energy-dispersive analysis of X-ray spectroscopy (EDX). Fourier transform-infrared (FTIR) spectral analysis of freeze-dried CELE-AgNPs was performed using an Alpha ATR Bruker spectrometer. Transmission electron microscopy (TEM) analysis was performed using a Philips CM200 device. The hydrodynamic diameter and electrokinetic

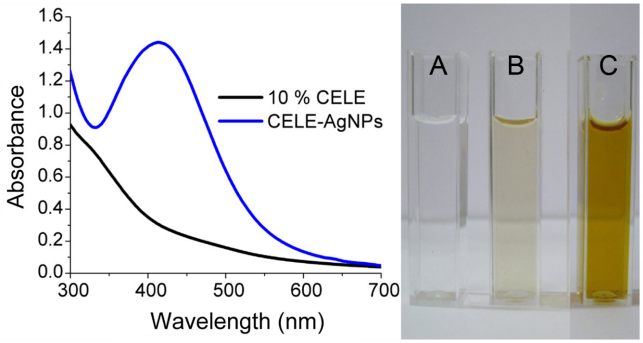

Fig. 1. Biosynthesis of *Canna edulis* leaf extract (CELE) and CELEsilver nanoparticles (AgNPs).
UV-visible spectroscopic analysis of CELE and CELE-AgNPs (left). Photographic image showing (A) $AgNO_3$, (B) CELE, and (C) CELE-AgNPs (right).

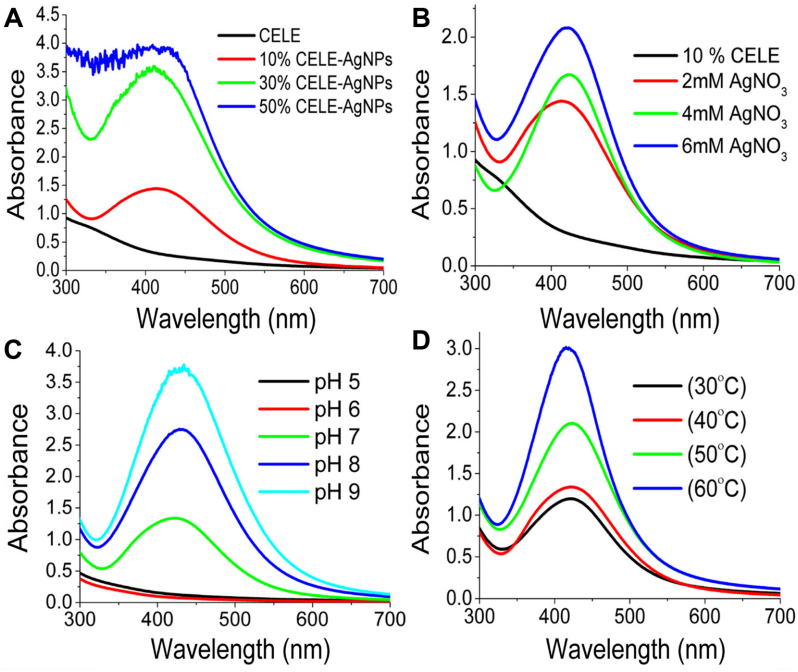

Fig. 2. UV-Vis spectroscopy of AgNPs synthesized using (**A**) different concentrations of *Canna edulis* leaf extract (CELE) with 2 mM $AgNO_3$, (**B**) different concentrations of $AgNO_3$ with 10% CELE, (**C**) at pH values ranging from 5 to 9, (**D**) and at temperatures ranging from 30°C to 60°C.

potential (zeta potential) of colloidal CELE-AgNPs were recorded using a NICOMP 380 ZIS device.

Results and Discussion

Biosynthesis of AgNPs

After incubating a mixture of 10 ml of CELE and 90 ml of 2 mM aqueous $AgNO_3$ for 24 h, a color change from brown to dark brown was observed. The surface plasmon resonance (SPR) properties of the CELE-AgNPs give a characteristic brown color to the colloidal solution [25, 26]. The absorbance peak observed at 410 nm in the UV-Vis spectrophotometric analysis confirmed formation of AgNPs using the leaf extract (Fig. 1). The right side of Fig. 1 shows the color change from brown to dark brown. The AgNPs are referred to as CELE-AgNPs, based on the source of the leaf extract. To study the effect of the CELE concentration on AgNP formation, different concentrations (10, 30, and 50 ml) of CELE were added to the 2 mM aqueous $AgNO_3$. As shown in Fig. 2A, as the concentration of CELE increased from 10 to 50 ml, the intensity of the peak at 410 nm also increased, due to an increase in the quantity of nanoparticles synthesized. The effect of the $AgNO_3$ concentration on AgNP synthesis was also studied, using 10 ml of CELE. As the $AgNO_3$ concentration increased from 2 to 6 mM, the peak red-shifted to 420 nm (Fig. 2B). This phenomenon is attributed to formation of larger nanoparticles [21]. No color change was observed in the aqueous solution of $AgNO_3$ alone, confirming the absence of abiotic formation of AgNPs. The effect of pH on the biosynthesis of CELE-AgNPs was observed by varying the pH from 5 to 9. As shown in Fig. 2C, the pH of the synthesis media affected the biosynthesis of AgNPs. No synthesis occurred at pH 5 or 6, as shown by the lack of absorption peaks at 410 nm. The SPR intensity increased as the pH of the extract increased from pH 7 to 9. Thus, synthesis of AgNPs using CELE requires a neutral or basic pH, and does not proceed at acidic pH. At neutral or basic pH, ionization of phenolic groups of compounds present in the leaf extract may have occurred, causing formation of AgNPs [5, 20, 27]. Although the reason for the lack of synthesis at acidic pH remains unclear, an acidic environment may inactivate the reducing functional groups. Under highly alkaline conditions, silver hydroxide may have formed. Thus, a neutral pH is most favorable for the synthesis of AgNPs. Temperature may also play a crucial role in the rapid synthesis of AgNPs using CELE. Fig. 2D shows the effects of temperature. As the temperature for synthesis rose from 30°C to 60°C, the

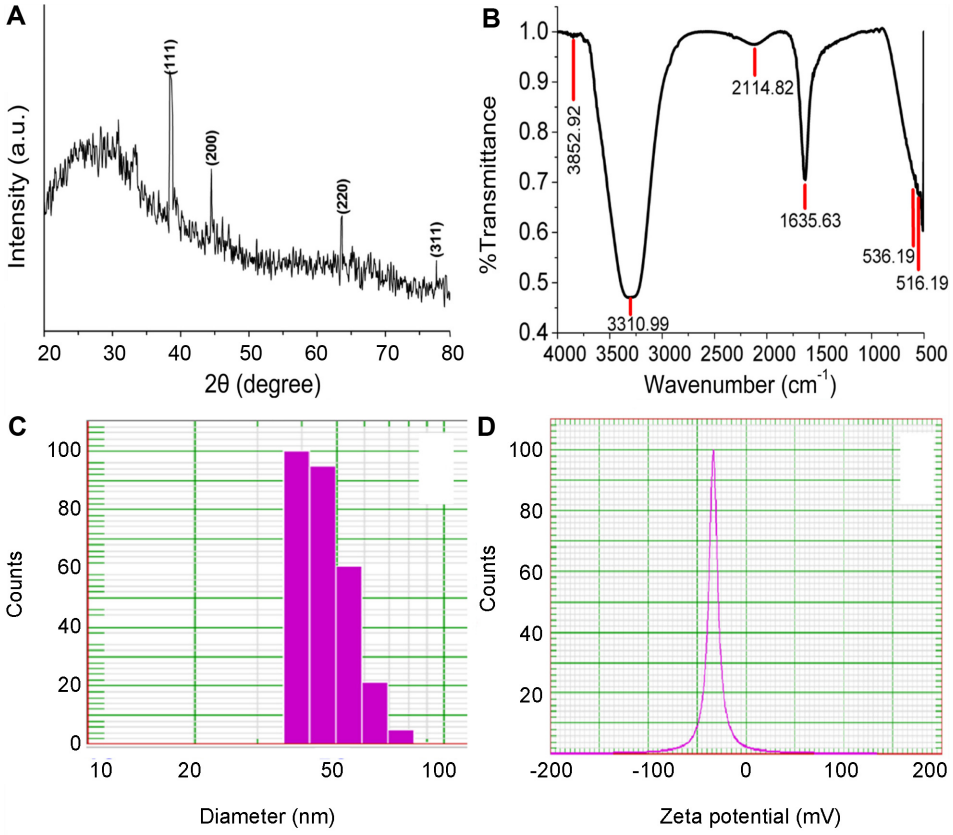

Fig. 3. (**A**) XRD analysis of *Canna edulis* leaf extract (CELE)-AgNPs, (**B**) FT-IR spectrum of CELE-AgNPs, (**C**) hydrodynamic diameter distribution of AgNPs in CELE, and (**D**) zeta potential measurement of AgNPs in CELE.

SPR intensity also increased, and the peak shifted towards a shorter wavelength, which is attributed to formation of smaller nanoparticles. Thus, a higher temperature induces more rapid reaction reduction of $AgNO_3$, leading to formation of smaller AgNPs.

CELE contains high concentrations of polyphenols, flavonoids, antioxidants, and proteins [22]. Phytochemicals extracted from the parenchyma of a *Cycas* leaf have been used in the synthesis of spherical AgNPs (2–6 nm) [28]. Whereas silver ions were reduced to AgNPs by proteins present in the leaf extract of *Capsicum annuum* L. [11], the biochemicals present in CELE contributed to the active conversion of aqueous $AgNO_3$ to CELE-AgNPs. The exact mechanism underlying the difference in the activities of the two cell-free extracts in reduction of $AgNO_3$ remains unclear, but it bears further investigation. Several plants have been tested for the biosynthesis of AgNPs under various reaction conditions. Bar *et al.* [15] and Jha and Prasad [28] reported heat-assisted biosynthesis of AgNPs using latex from *Jatropha curcus* and *Cycas* leaf extract, respectively. Kéki *et al*. [29] demonstrated UV light–assisted synthesis of AgNPs. However, no external heat or light was required for synthesis of nanoparticles using our method, and the synthesis of CELE-AgNPs occurred at ambient temperature and under neutral reaction conditions.

Characterization of AgNPs

The SPR peak observed by UV-Vis spectrophotometry at 410 nm indicates the presence of spherical nanoparticles (Fig. 1) [30]. Fig. 3A shows the XRD pattern of CELE-AgNPs with a Cu K_α target in the 0–100° range. Four peaks were observed in the XRD pattern, at 2θ values of 37.8°, 44.1°, 62.9°, and 75.9°, and were indexed as (111), (200), (220), and (311), respectively, which confirms a face centric cubic crystal structure [31]. The obtained pattern corresponds with JCPDF Card No. 04-0783. From the Debye–Sherrer formula, $D = 0.9\lambda/\beta\cos\theta$ (β = full width at half maximum, λ = X-ray wavelength of the Cu target (1.54 Å), D = average crystal size, and θ = diffraction angle). For measurement of the crystal size of the nanoparticles, Gaussian fitting of each peak was performed. From the formula, the CELE-AgNPs showed a crystal size of 15 nm, which was

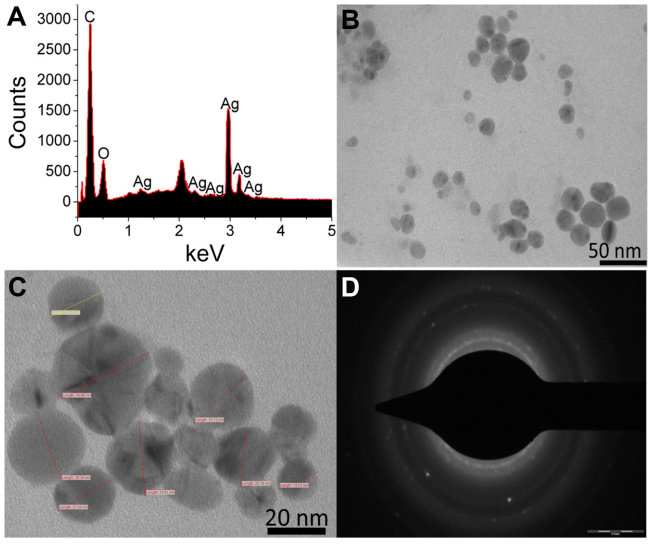

Fig. 4. (**A**) EDS spectra of freeze-dried *Canna edulis* leaf extract-AgNPs, (**B**, **C**) TEM images of AgNPs at different magnifications, and (**D**) SAED pattern of as-synthesized AgNPs.

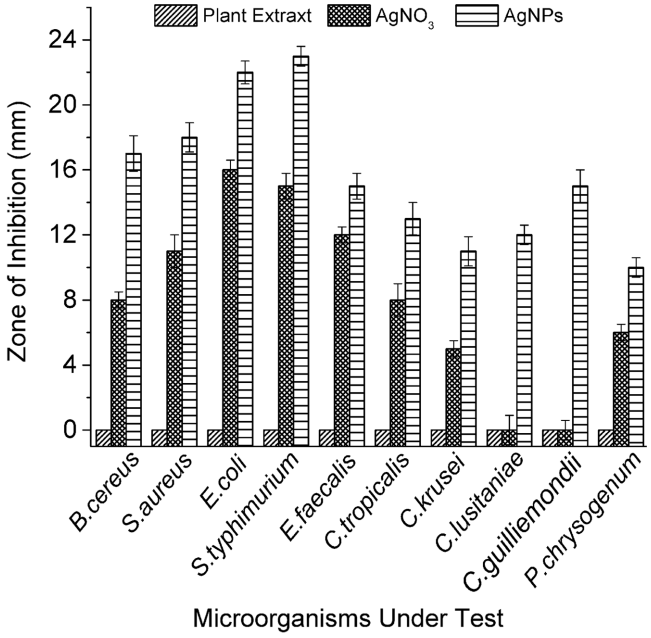

Fig. 5. Antimicrobial activity of *Canna edulis* leaf extract (CELE), $AgNO_3$, and CELE-AgNPs against pathogenic microorganisms as measured using a zone of inhibition (mm).

concordant with the results of TEM analysis.

The interaction between the CELE biomolecules responsible for reduction and stabilization of silver ions into AgNPs was evaluated using FT-IR measurement of freeze-dried CELE-AgNPs. Various biomolecules, including polyphenols, flavonoids, carbohydrates, proteins, and peptides, are present in the leaf extract. In the IR region of the electromagnetic spectrum, vibrations characteristic of amino acid residues of proteins or peptides were observed, at ~1,635 and 2,114 cm^{-1}. In addition, corresponding vibrations were observed at ~3,310 and 3,850 cm^{-1} (Fig. 3B). Cysteine residues or free amine groups and negatively charged carboxylate groups of proteins are thought to be involved in the protein–nanoparticle interaction [32–34]. The results indicate that a protein carbonyl group interacts with the metal nanoparticles, indicating the presence of proteins playing significant roles in the formation of the AgNPs and in preventing aggregation. The hydrodynamic distribution (Fig. 3C) and zeta potential (Fig. 3D) of the colloidal AgNPs were 40 ± 5 nm and −33.7 mV, respectively, indicating that the particles are nanometer-sized and have excellent stability in suspension [35]. EDX analysis was performed for the compositional study, which showed typical signals of elemental silver at 3 keV (Fig. 4A) [16]. The TEM results also confirmed the presence of spherical, polydispersed CELE-AgNPs with 25 nm average size (Figs. 4B and 4C). The SAED pattern obtained is characteristic of elemental silver, indicating formation of crystalline AgNPs (Fig. 4D).

Antimicrobial Activity

Although various mechanisms have been proposed for the bactericidal activity of AgNPs, the mechanism of action remains undetermined. Various papers have stated that the integrity of the bacterial cell membrane is disturbed by attachment of AgNPs, which disrupts the respiratory machinery of the cells, allowing the nanoparticles to enter the cells [36, 37]. Small nanoparticles have a larger collective surface area than large nanoparticles, which facilitates greater interaction between small nanoparticles and microorganisms, producing a stronger bactericidal effect [18, 38]. The strength of nanoparticle-mediated antimicrobial activity also depends on the shape of the nanoparticles [39, 40].

Although CELE has mild antimicrobial activity, no antimicrobial activity was observed against the human pathogenic microorganisms tested. The antimicrobial activity of aqueous $AgNO_3$ was compared with that of as-prepared AgNPs. CELE-AgNPs showed strong antimicrobial activity against all microorganisms tested, including gram-negative and gram-positive bacteria, and several fungal species; the antimicrobial activity of CELE-AgNPs was stronger than that of $AgNO_3$ (Fig. 5). Gram-negative bacteria showed stronger resistance to the nanoparticles than gram-positive bacteria, perhaps owing to differences in cell wall architecture. The fungal species were resistant to aqueous $AgNO_3$ but

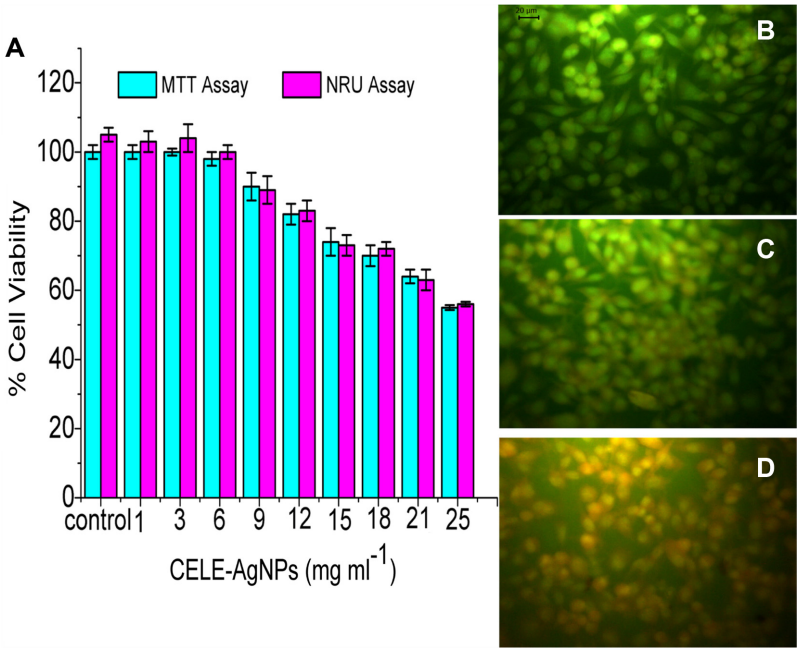

Fig. 6. In vitro cytotoxicity of different concentrations of AgNPs, as tested on the L929 cell line.
(**A**) MTT assay (blue bars), and NRU assay (pink bars). (**B**–**D**) fluorescence microscopic images of L929 cells exposed to various concentrations; (**B**) control, (**C**) 18 μg/ml (~IC_{50}), and (**D**) 25 μg/ml (~2 × IC_{50}).

were susceptible to CELE-AgNPs. Thus, the as-prepared AgNPs showed potential antimicrobial activity. However, before these particles can be applied to uses in biomedical or industrial fields, their cytotoxicity to mammalian cells must be tested against mammalian cells.

In Vitro Cytotoxicity

AgNPs have been extensively studied and they have been demonstrated to show potent antimicrobial activity. Despite this major advantage, they have also been shown to affect mammalian cells. Therefore, to determine the toxicity of CELE-AgNPs to cells, the in vitro cytotoxicity of AgNPs was tested on the L929 cell line using an MTT assay (Fig. 6A; blue bars) and an NRU assay (Fig. 6A; pink bars). In both assays, as the concentration of CELE-AgNPs increased, the toxicity of the nanoparticles towards the L929 cells increased (Figs. 6B–6D). After 24 h of incubation at concentrations of 1.5, 3.12, and 6.25 μg/ml, the AgNPs showed no significant effect, whereas concentrations greater than 12.5 μg/ml affected cell viability.

The toxicity of AgNPs to cells was investigated using a simple and rapid fluorescence microscopy method, using AO/EB (nucleus binding dyes) staining for observation of necrotic and apoptotic effects. AO stain penetrates all cells, and stains the nuclei green. Cells with membrane damage can take up only EB, which stains the nucleus red. The EB stain is dominant to the AO stain. Therefore, live cells exhibit a green nucleus; cells with a bright green nucleus are designated as early apoptotic cells; late apoptotic cells exhibit orange chromatin; structurally normal orange chromatin is observed in cells that have undergone necrosis [41]. Concentrations of 0 μg/ml (control), 18 μg/ml (~IC_{50}), and 25 μg/ml (~2 × IC_{50}) were used. Figs. 6B–6D show fluorescence microscopic images of L929 cells exposed to the above concentrations. Intact cells and their nuclei could be visualized in control cells (Fig. 6B). The cells exposed to ~IC_{50} and ~ 2 × IC_{50} AgNPs showed fragmented nuclei and nonviable nuclei, respectively (Figs. 6C and 6D). Apoptotic cells did not show any adverse effects. Thus, the IC_{50} concentration is appropriate for biomedical applications. These results demonstrate that the nanoparticles show a dose-dependent cytotoxic effect on mammalian cells. In addition, the concentration required to inhibit growth of microorganisms is less than the dose that causes 50% growth inhibition of a mammalian cell line. CELE contains abundant phytochemicals, and their presence on the CELE-AgNPs would have increased the cytocompatibility. Further modification of the process is required to make these nanoparticles applicable to medicinal uses. The potential interactions of CELE-AgNPs with normal animal cell lines

and cancerous cells require additional investigation for better risk assessment.

In conclusion, we have described a promising green chemistry approach to the biosynthesis of metal nanostructures. The leaf extract of the flowering plant *C. edulis* Ker-Gawl. was demonstrated to show potential for use in eco-friendly, green synthesis of AgNPs. The CELE-AgNPs were crystalline and <40 nm in size. The as-prepared nanoparticles had excellent stability in colloidal solution. These AgNPs were found to possess promising antimicrobial activity against pathogenic microorganisms. The biocompatibility of these AgNPs was tested in a mammalian cell line, and showed dose-dependent cytotoxicity. The AO/EB staining method was used for assessment of apoptosis and necrosis in mammalian cells following treatment with CELE-AgNPs. The IC_{50} concentration for the mammalian cells was greater than that required for inhibition of the pathogenic microbial cells. Therefore, CELE shows potential for use in green synthesis of AgNPs.

Acknowledgments

This research was supported by the 2015 KU Brain Pool Fellowship of Konkuk University, Republic of Korea. We are grateful to the Department of Microbiology, Department of Biochemistry, and Department of Biotechnology, Shivaji University, Kolhapur for allowing us to use their facilities. This paper was also supported by the KU Research Professor Program of Konkuk University.

References

1. Kim TS, Patel SKS, Selvaraj C, Jung WS, Pan CH, Kang YC, Lee J-K. 2016. A highly efficient sorbitol dehydrogenase from *Gluconobacter oxydans* G624 and improvement of its stability through immobilization. *Sci. Rep.* **6**: 33438.
2. Patel SKS, Jeong J-H, Mehariya S, Otari SV, Madan B, Haw JR, *et al*. 2016. Production of methanol from methane by encapsulated *Methylosinus sporium*. *J. Microbiol. Biotechnol.* **26:** 2098-2105.
3. Patel SKS, Choi SH, Kang YC, Lee JK. 2016. Large-scale aerosol-assisted synthesis of biofriendly Fe_2O_3 yolkshell particles: a promising support for enzyme immobilization. *Nanoscale* **8:** 6728-6738.
4. Patel SKS, Mardina P, Kim S-Y, Lee J-K, Kim I-W. 2016. Biological methanol production by a type II methanotroph *Methylocystis bryophila*. *J. Microbiol. Biotechnol.* **26:** 717-724.
5. Patel SKS, Mardina P, Kim D, Kim S-Y, Kalia VC, Kim I-W, Lee J-K. 2016. Improvement in methanol production by regulating the composition of synthetic gas mixture and raw biogas. *Bioresour. Technol.* **218:** 202-208.
6. Vorobyova SA, Lesnikovich AI, Sobal NS. 1999. Preparation of silver nanoparticles by interphase reduction. *Colloids Surf. A Physicochem. Eng. Asp.* **152:** 375-379.
7. Dahl JA, Maddux BLS, Hutchison JE. 2007. Toward greener nanosynthesis. *Chem. Rev.* **107:** 2228-2269.
8. Dimitrijevic NM, Bartels DM, Jonah CD, Takahashi K, Rajh T. 2001. Radiolytically induced formation and optical absorption spectra of colloidal silver nanoparticles in supercritical ethane. *J. Phys. Chem. B* **105:** 954-959.
9. Petit C, Lixon P, Pileni MP. 1993. In-situ synthesis of silver nanocluster in AOT reverse micelles. *J. Phys. Chem.* **97:** 12974-12983.
10. Lee J-K, Kim I-W, Kim T-S, Choi J-H, Kim J-H, Park S-H. 2014. Immunological activities of cationic methylan derivatives. *J. Kor. Soc. Appl. Biol. Chem.* **57:** 319-321.
11. Li S, Shen Y, Xie A, Yu X, Qiu L, Zhang L. 2007. Green synthesis of silver nanoparticles using *Capsicum annuum* L. extract. *Green Chem.* **9:** 852-858.
12. Sandmann G, Dietz H, Plieth W. 2000. Preparation of silver nanoparticles on ITO surfaces by a double-pulse method. *J. Electroanal. Chem.* **491:** 78-86.
13. Patel SKS, Kalia VC, Choi JH, Haw JR, Kim IW, Lee JK. 2014. Immobilization of laccase on SiO_2 nanocarriers improves its stability and reusability. *J. Microbiol. Biotechnol.* **24:** 639-647.
14. Smetana AB, Klabunde KJ, Sorensen CM. 2005. Synthesis of spherical silver nanoparticles by digestive ripening, stabilization with various agents, and their 3-D and 2-D superlattice formation. *J. Colloid Interface Sci.* **284:** 521-526.
15. Bar H, Bhui DK, Sahoo GP, Sarkar P, Sankar PD, Misra A. 2009. Green synthesis of silver nanoparticles using latex of *Jatropha curcas*. *Colloids Surf. A Physicochem. Eng. Asp.* **339:** 134-139.
16. Mardina P, Li J, Patel SKS, Kim I-W, Lee J-K, Selvaraj C. 2016. Potential of immobilized whole-cell *Methylocella tundrae* as a biocatalyst for methanol production from methane. *J. Microbiol. Biotechnol*. **26:** 1234-1241.
17. Magudapathy P, Gangopadhyay P, Panigrahi BK, Nair KGM, Dhara S. 2001. Electrical transport studies of Ag nanoclusters embedded in glass matrix. *Physica B Condens. Matter* **299:** 142-146.
18. Morones JR, Elechiguerra JL, Camacho A, Holt K, Kouri JB, Ramírez JT, Yacaman MJ. 2005. The bactericidal effect of silver nanoparticles. *Nanotechnology* **16:** 2346-2353.
19. Zhao Z, Ramachandran P, Choi JH, Lee J-K, Kim I-W. 2013. Purification and characterization of a novel β-1,3/1,4-glucanase from *Sistotrema brinkmannii* HQ717718. *J. Kor. Soc. Appl. Biol. Chem.* **56:** 263-270.
20. Kumar V, Yadav SK. 2008. Plant-mediated synthesis of silver and gold nanoparticles and their applications. *J. Chem. Technol. Biotechnol*. **84:** 151-157.
21. Naik RR, Stringer SJ, Agarwal G, Jones SE, Stone MO. 2002. Biomimetic synthesis and patterning of silver nanoparticles.

Nat. Mater. **1:** 169-172.
22. Zhang J, Wang ZW, Mi Q. 2011. Phenolic compounds from *Canna edulis* Ker residue and their antioxidant activity. *LWT Food Sci. Technol*. **44:** 2091-2096.
23. Woradulayapinij W, Soonthornchareonnon N, Wiwat C. 2005. In vitro HIV type 1 reverse transcriptase inhibitory activities of Thai medicinal plants and *Canna indica* L. rhizomes. *J. Ethnopharmacol*. **101:** 84-89.
24. Cui L, Ouyang Y, Lou Q, Lou Q, Yang F, Chen Y, Zhu W, Luo S. 2010. Removal of nutrients from wastewater with *Canna indica* L. under different vertical-flow constructed wetland conditions. *Ecol. Eng*. **36:** 1083-1088.
25. Otari SV, Yadav HM, Thorat HM, Patil RM, Lee JK, Pawar SH. 2016. Facile one pot synthesis of core shell Ag@SiO_2 nanoparticles for catalytic and antimicrobial activity. *Mater. Lett.* **167:** 179-182.
26. Otari SV, Patil RM, Nadaf NH, Ghosh SJ, Pawar SH. 2012. Green biosynthesis of silver nanoparticles from an actinobacteria *Rhodococcus* sp. *Mater. Lett.* **72:** 92-94.
27. Patel SKS, Selvaraj C, Mardina P, Jeong J-H, Kalia VC, Kang Y-C, Lee J-K. 2016. Enhancement of methanol production from synthetic gas mixture by *Methylosinus sporium* through covalent immobilization. *Appl. Energy* **171:** 383-391.
28. Jha AK, Prasad K. 2010. Green synthesis of silver nanoparticles using *Cycas* Leaf. *Int. J. Green Nanotechnol. Phys. Chem*. **1:** 110-117.
29. Kéki S, Török J, Deák G, Daróczi L, Zsuga M. 2000. Silver nanoparticles by PAMAM-assisted photochemical reduction of Ag(+). *J. Colloid Interface Sci*. **229:** 550-553.
30. Otari SV, Patil RM, Nadaf NH, Ghosh SJ, Pawar SH. 2014. Green synthesis of silver nanoparticles by microorganism using organic pollutant: its antimicrobial and catalytic application. *Environ. Sci. Pollut. Res*. **21:** 1503-1513.
31. Shetty PR, Kumar BS, Kumar YS, Shankar GG. 2012. Characterization of silver nanoparticles synthesized by using marine isolate *Streptomyces albidoflavus*. *J. Microbiol. Biotechnol*. **22:** 614-621.
32. Gole A, Dash C, Ramakrishnan V, Sainkar SR, Mandale AB, Rao M, Sastry M. 2001. Pepsin-gold colloid conjugates: preparation, characterization, and enzymatic activity. *Langmuir* **17:** 1674-1679.
33. Sastry M, Mayya KS, Bandyopadhyay K. 1997. pH Dependent changes in the optical properties of carboxylic acid derivatized silver colloidal particles. *Colloids Surf. A Physicochem. Eng. Asp*. **127:** 221-228.
34. Ramachandran P, Jagtap SS, Patel SKS, Li J, Kang YC, Lee J-K. 2016. Role of the non-conserved amino acid asparagine 285 in the glycone-binding pocket of *Neosartorya fischeri* β-glucosidase. *RSC Adv.* **6:** 48137-48144.
35. Malvern Instruments. 2011. Zeta potential: an introduction in 30 minutes. *Zetasizer Nano Series Tech. Note MRK654-01*. **2:** 1-6.
36. Dhanasekar NN, Rahul GR, Narayanan KB, Raman G, Sakthivel N. 2015. Green chemistry approach for the synthesis of gold nanoparticles using the fungus *Alternaria* sp. *J. Microbiol. Biotechnol.* **25:** 1129-1135.
37. Kvítek L, Panáček A, Soukupová J, Kolář M, Večeřová R, Prucek R, *et al*. 2008. Effect of surfactants and polymers on stability and antibacterial activity of silver nanoparticles. *J. Phys. Chem. C* **112:** 5825-5834.
38. Jena J, Pradhan N, Nayak RR, Dash BP, Sukla LB, Panda PK, Mishra BK. 2014. Microalga *Scenedesmus* sp.: a potential low-cost green machine for silver nanoparticle synthesis. *J. Microbiol. Biotechnol.* **24:** 522-533.
39. Pal S, Tak YK, Song JM. 2007. Does the antibacterial activity of silver nanoparticles depend on the shape of the nanoparticle? A study of the gram-negative bacterium *Escherichia coli*. *Appl. Environ. Microbiol*. **73:** 1712-1720.
40. Otari SV, Patel SKS, Jeong JH, LeeJH, Lee JK. 2016. A green chemistry approach for synthesizing thermostable antimicrobial peptide-coated gold nanoparticles immobilized in an alginate biohydrogel. *RSC Adv.* **6:** 86808-86816.
41. Renvoize C, Biola A, Pallardy M, Bre J. 1998. Apoptosis: identification of dying cells. *Cell Biol. Toxicol.* **14:** 111-120.